ENVIRONMENTAL RESEARCH
LETTERS

PURPOSE-LED PUBLISHING™

Celebrating the 20th anniversary of Environmental Research Letters

LETTER • OPEN ACCESS

Arctic sea ice loss drives enhanced East Asian summer temperature variability

To cite this article: Doo Young Lee *et al* 2026 *Environ. Res. Lett.* **21** 084015

View the article online for updates and enhancements.

You may also like

- A recent weakening of winter temperature association between Arctic and Asia
Bingyi Wu, Zhenkun Li, Jennifer A Francis et al.
- A surface temperature dipole pattern between Eurasia and North America triggered by the Barents–Kara sea-ice retreat in boreal winter
Yurong Hou, Wenju Cai, David M Holland et al.
- Strengthened impact of late autumn Arctic sea ice on Asian winter cold extremes after 1999/2000
Cen Wang, Hui Su, Jianqiu Zheng et al.

This content was downloaded from IP address 203.255.190.41 on 22/09/2026 at 02:26

ENVIRONMENTAL RESEARCH
LETTERS

Check for updates

OPEN ACCESS

RECEIVED
9 February 2026

REVISED
1 April 2026

ACCEPTED FOR PUBLICATION
14 April 2026

PUBLISHED
24 April 2026

Original content from this work may be used under the terms of the Creative Commons Attribution 4.0 licence.

Any further distribution of this work must maintain attribution to the author(s) and the title of the work, journal citation and DOI.

LETTER

Arctic sea ice loss drives enhanced East Asian summer temperature variability

Doo Young Lee[1], **Sang-Wook Yeh**[1,*], **Yong-Han Lee**[2], **Guojian Wang**[3,4,5], **Shangfeng Chen**[6] and **Renguang Wu**[7]

[1] Department of Climate and Energy Systems Engineering, Ewha Womans University, Seoul, Republic of Korea
[2] Department of Marine Science and Convergence Engineering, Hanyang University, Ansan, Republic of Korea
[3] Frontier Science Center for Deep Ocean Multispheres and Earth System (FDOMES) and Physical Oceanography Laboratory, Ocean University of China, Qingdao 266100, People's Republic of China
[4] Laoshan Laboratory, Qingdao, People's Republic of China
[5] Institute of Marine Science and Technology, Shandong University, Qingdao 266237, People's Republic of China
[6] State Key Laboratory of Earth System Numerical Modeling and Application, Institute of Atmospheric Physics, Chinese Academy of Sciences, Beijing, People's Republic of China
[7] Department of Atmospheric Sciences, School of Earth Sciences, Zhejiang University, Hangzhou, People's Republic of China
* Author to whom any correspondence should be addressed.

E-mail: swyeh@ewha.ac.kr

Keywords: Arctic sea ice variability, East Asian summer temperature variability, dipole-like circulation, Arctic–midlatitude teleconnection

Supplementary material for this article is available online

Abstract

This study investigates the link between enhanced Arctic sea ice (ASI) variability and increased summer temperature variability over East Asia since the early 2000s. We find that the rate of ASI decline has accelerated during this period, accompanied by a near doubling of its interannual variability. This heightened variability is associated with a reorganization of Arctic atmospheric circulation, characterized by the increased prominence and intensified variability of a dipole-like mode. This mode is strongly correlated with the marked increase in summer surface temperature variability across East Asia. The underlying mechanism involves the dipole-like mode driving pronounced meridional shifts in the East Asian jet stream, which reshape the upper-tropospheric structure and generate opposing cooling and warming anomalies, thereby amplifying regional temperature contrasts. These results indicate that the loss of ASI affects not only the mean-state of Arctic circulation but also enhances its dynamical variability, strengthening Arctic–midlatitude teleconnections and increasing the likelihood of extreme climate events. Our findings highlight summer ASI variability as a critical factor influencing midlatitude climate variability and prediction uncertainty, underscoring its importance for future seasonal forecasts and long-term climate risk assessments in East Asia.

1. Introduction

Arctic sea ice (ASI) plays a key regulatory role in the Earth's climate system [1–6]. Since the early 2000s, numerous studies have reported a rapid and sustained decline in ASI [7–9]. This reduction, occurring across all seasons, has had profound and widespread impacts on the global climate system. As a consequence, increasing scientific attention has been directed toward understanding the implications of ASI loss, including Arctic amplification, changes in atmospheric circulation, and their emerging teleconnections with extreme weather and climate events in mid-latitude regions [3, 8, 10–12].

In summer, the decline in ASI has become particularly pronounced, driven largely by the accelerated warming of Arctic sea surface temperatures (SSTs) under global warming. Compared with the period before the 2000s, the rate of summer sea ice loss has increased substantially since the 2000s [8, 13, 14]. This rapid retreat has led to notable changes in Arctic atmospheric circulation [15, 16], which can, in turn, serve as a potential driver of extreme weather and climate events in the midlatitudes, including

© 2026 The Author(s). Published by IOP Publishing Ltd

severe heat waves, droughts, floods, and wildfires [16–19]. Indeed, there has been increasing interest in understanding how changes in summer Arctic atmospheric circulation influence temperature and precipitation patterns in the mid-latitudes, including East Asia [2, 20–22]. Notably, the interannual variability of summer surface temperatures across East Asia has shown a remarkable increasing trend since the 2000s [20, 23, 24]. This enhanced surface temperature variability is closely related to greater forecast uncertainty, which poses substantial challenges for decision-making and the development of effective response strategies across various sectors, including public policy, urban planning, and socioeconomic risk management.

In this context, it is particularly noteworthy that not only has the overall decline in ASI occurred since the 2000s, but its variability has also increased markedly [7, 16, 25–27]. While previous studies have explored the impacts of summer ASI loss on mid-latitude climate, relatively little is known about the extent to which the enhanced summer ASI variability itself contributes to the observed increase in summer temperature variability. Improving our understanding of the characteristics and underlying mechanisms of this variability is essential for enhancing preparedness for future climate risks and ensuring the resilience of socio-economic systems. Recent studies have also demonstrated that incorporating realistic ASI conditions can enhance seasonal prediction skill not only within the Arctic but also across mid-latitude regions, including Eurasia, highlighting the importance of Arctic variability in modulating large-scale climate predictability (e.g. [28]). Accordingly, this study aims to elucidate the physical mechanisms behind the intensified summer ASI variability and to investigate its connection to the increasing surface temperature variability over East Asia. Unless otherwise specified, the analysis focuses on the boreal summer (June to August, JJA), using both observational datasets and idealized model experiments in which SSTs are prescribed only over the Arctic Ocean to isolate the direct climate impact attributed to SST forcing in the Arctic.

2. Data and methods

2.1. Reanalysis dataset

Monthly net surface heat flux (NSHF), mean sea level pressure (MSLP), air temperature, zonal and meridional wind, vertical velocity, and geopotential heights were obtained from the fifth-generation ECMWF reanalysis (ERA5) [29] for 1980–2022 at a global spatial resolution 1° × 1°. Monthly SST data were taken from NOAA's Extended Reconstructed SST version 5 (ERSST v5) [30], and sea ice concentration (SIC) data were provided by NOAA/NSIDC [31]. ASI extent (SIE) was calculated by summing grid cells with SIC exceeding 15% north of 70°N. Summer anomalies were computed relative to the 1980–1999 climatology.

2.2. Climate regime analysis

The classification of the regime into two periods, the pre-2000s and post-2000s, is based on the objective identification of a climate-induced regime shift in area-averaged JJA SIC north of 70°N during 1980–2022. The primary detection used a sequential regime shift detection algorithm [32], which is well suited for identifying climate regime transitions in long time series (figure S1). To assess robustness, we also applied the Pettitt test [33], a widely used non-parametric change-point detection method (figure S1). Both methods yield highly consistent regime transitions across multiple Arctic climate variables (figure 1 for the sequential algorithm and figure S2 for the Pettitt test). Accordingly, the regime shift identified by the sequential algorithm, occurring around 2000, is adopted as the basis for the analyses presented in this study.

2.3. Empirical orthogonal function (EOF) analysis

To investigate the characteristics of summer atmospheric structural changes in the Arctic region, EOF [34] analysis was applied to JJA MSLP anomalies over the Arctic domain (60–90 °N), with cosine latitude weighting, for both observations and model simulations. EOFs were computed from temporally anomalous fields derived from the ensemble means of 30 members per year to extract the dominant mode of internal atmospheric variability.

2.4. GFDL-CM2.1 simulations

To account for atmosphere–ocean feedbacks that are absent in atmosphere-only experiments [35], we conducted idealized ensemble simulations using Geophysical Fluid Dynamics Laboratory Climate Model version 2.1 (GFDL-CM2.1) [36], in line with previous studies [37–39] that emphasizes the importance of incorporating atmosphere-ocean interaction processes when investigating Arctic variability. The model consists of atmosphere, ocean, land, and sea ice components. The atmospheric and land components use a horizontal resolution of 2° × 2.5° (latitude × longitude), with 24 vertical atmospheric levels. The ocean and sea ice components are based on a 200 × 360 tripolar grids in latitude-longitude, with 50 vertical ocean levels. Thirty ensemble members were integrated with different initial conditions. Specifically, each ensemble member was initialized from distinct atmospheric and oceanic states extracted from a long-term control integration of GFDL-CM2.1, thereby sampling different realizations of internal climate variability. No additional perturbations were imposed, and the ensemble spread arises solely from differences in the initial conditions of the fully coupled system, including the atmosphere, ocean, sea ice, and land components. To investigate

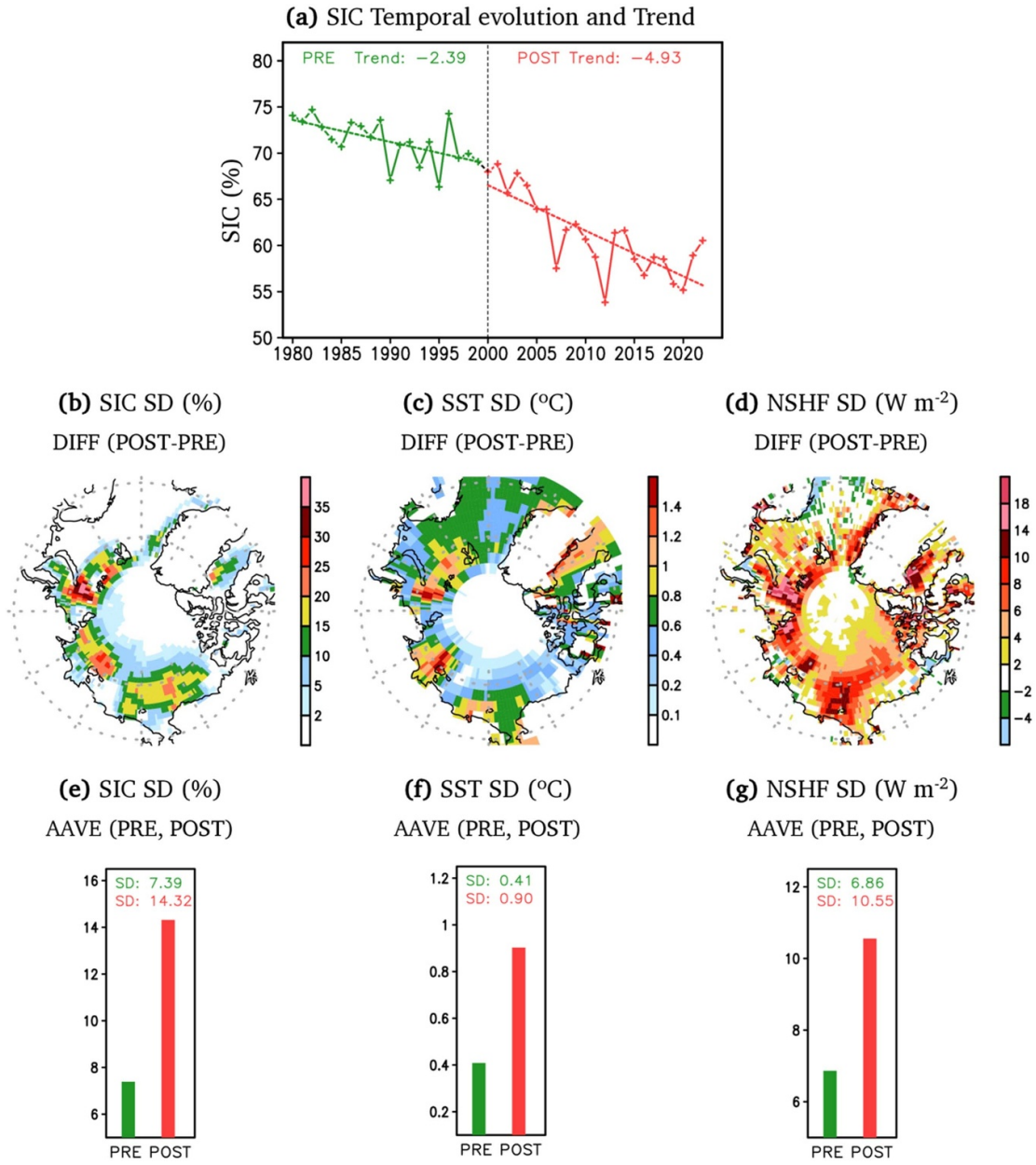


Figure 1. Change in summer Arctic sea ice variability between the pre-2000s (1980–1999) and post-2000s (2000–2022). (a), Temporal evolution (%) and trend (% decade^{-1}) of summer (June to August, JJA) Arctic sea ice concentration (SIC) averaged over the Arctic (70°–90 °N, 0°–360 °E) during the pre-2000s (1980–1999) and post-2000s (2000–2022). Both trends are statistically significant at a 90% confidence level based on a two-tailed Student's *t*-test. Trend values (% decade^{-1}) are displayed at the top of the panel. (b)–(d), Differences in the standard deviations (SDs) of JJA SIC (%), sea surface temperature (SST; °C), and net surface heat flux (NSHF; W m^{-2}) between the post-2000s and pre-2000s, respectively. (e)–(g), JJA SDs of SIC, SST, and NSHF averaged over the Arctic (70°–90 °N, 0°–360 °E) during the pre-2000s and post-2000s.

the effect of Arctic warming, SSTs north of 65 °N were restored to observed historical daily SSTs (1951–2022) from NOAA ERSST version 3b [40] using a 5 day relaxation (or nudging) time scale (referred to as the ARCTIC_run). This configuration reasonably reproduces the observed ASI decline, although it tends to underestimate both its magnitude and internal variability (figure S3). Atmospheric CO_2 concentration is fixed at 353 ppm (1989 level) to isolate the response of the Arctic warming associated with sea ice loss by minimizing the influence of anthropogenic warming. The simulated SIC rapidly adjusts to the observed SST evolution while maintaining thermodynamic balance with the restored SSTs in the Arctic. Outside the SST-restored region, fully coupled interactions among the ocean, atmosphere, and sea ice occur without SST restoration. This experimental configuration has been used in previous studies [41, 42] to investigate the effects of Arctic warming. A parallel control simulation (referred to as CLIM_run) was also conducted under the same conditions as the ARCTIC_run, except for using the observed climatological SSTs (1951–2016). Anomalies were defined as ARCTIC_run minus CLIM_run for each

corresponding year and variable to reduce potential systematic biases inherent in the model and isolate the effects of Arctic warming associated with sea ice loss. All outputs were regridded to a global spatial resolution of 1° × 1°, and the analysis focus on 1980–2022.

2.5. Statistical analysis

Linear trends and regression coefficients were estimated using least-squares regression, including regressions onto EOF principal component (PC) time series. Variability was quantified using standard deviation and 11 year sliding variance of either PCs or regional mean time series of the climate variables. Temporal correlation coefficients (TCCs) are calculated to quantify the temporal relationships between two time series. Statistical significance was assessed using a two-tailed Student's *t*-test at the 90% or 95% confidence level [43]. Pattern similarity was evaluated using pattern correlation coefficients with latitude weighting.

3. Results

3.1. Increased variability of summer ASI since the 2000s

Observed Arctic SIC, averaged over 70°–90 °N across all longitudes, shows year-to-year variation since 1980, accompanied by a pronounced long-term decline (figure 1(a)). In particular, the rate of Arctic SIC decline becomes more pronounced after the 2000s (post-2000s, hereafter) compared to the period before the 2000s (pre-2000s, hereafter). This is demonstrated by the results of the climate regime analysis (see section 2 for details), which divides the period at the year 2000 and reveals that the Arctic SIC decreased at rates of 2.39% per decade during the pre-2000s and 4.93% per decade during the post-2000s (figure 1(a)).

Spatial distribution analysis of Arctic SIC trends from 2000 to 2022 (figure S4(a)) reveals a widespread decrease across the Arctic, with particularly pronounced reductions in the Kara and Laptev Seas. In contrast, observed SSTs in these regions indicate a pronounced warming trend, suggesting that elevated SSTs are contributing to the decline in Arctic SIC (figure S4(b)). Furthermore, these regions coincide with areas showing a marked increase in NSHF from the atmosphere to the ocean, supporting the interpretation that the SST anomalies are primarily driven by atmospheric circulation anomalies (figure S4(c)). However, the resultant SST anomalies can in turn exert strong feedback on the overlying atmospheric circulation, potentially amplifying mid-latitude climate anomalies. These results therefore underscore not only the role of atmospheric forcing but also the importance of Arctic sea-ice–atmosphere coupling in shaping the observed changes. Meanwhile, over the Russian continent, Alaska, and northwestern Canada, regions surrounding the Arctic Ocean, the NSHF shows a weak but noticeable upward heat transport toward the atmosphere. This pattern is primarily driven by the northward advection of warm air from the continent and is consistent with previous findings [44], which suggest that enhanced downward heat flux from the atmosphere to the ocean contributes to the reduction of ASI. It is noteworthy that, in addition to the long-term trends of each variable (figure S4), their variability has also markedly increased since the 2000s, particularly in regions that experienced large changes (figures 1(b)–(d) and S5). These results are consistent with previous studies [7, 16, 25–27], which suggest that greater declines in ASI are typically accompanied by enhanced variability. Furthermore, when comparing the area-averaged variability of each variable over the Arctic region (70°–90 °N, 0°–360 °E), the post-2000s shows nearly a twofold increase relative to the pre-2000s, by factors of 1.94, 2.20, and 1.54 for SIC, SST, and NSHF, respectively (figures 1(e)–(g)).

3.2. Changes in the dominant atmospheric structure and its variability over the Arctic

To examine the primary structures of large-scale atmospheric circulation over the Arctic, we conducted an EOF analysis using summer MSLP anomaly from 1980 to 2022.

The first EOF mode reveals a summer Arctic Oscillation (AO)-like pattern (figure S6(a)), which tends to persist over time, although it has weaker intensity and smaller spatial extent compared to the winter AO pattern [45–48]. The second and third EOF modes display tripole-like (figure S6(b)) and dipole-like (figure S6(c)) circulation patterns, respectively. This distinctive feature of Arctic atmospheric circulation exhibits an inter-mode transition around the 2000s. While the AO-like pattern does not show significant differences between the two periods (figures S6(d) and (g)), the tripole-like and dipole-like modes display a distinct role-exchanging behavior. For instance, the tripole-like pattern appeared as the second EOF mode before the 2000s (figure S6(e)), but shifted to the third mode after the 2000s (figure S6(i)). In contrast, the dipole-like pattern emerged as the second mode in the post-2000s (figures S6(f) and (h)). Although these patterns are not perfectly symmetrical, they retain a highly similar structure, which is quantitatively supported by the correlation coefficients between the respective patterns (table S1). This serves as evidence for a structural transition in the Arctic atmospheric circulation modes around the 2000s. Furthermore, the strong correlation between the PC time series of the tripole-like mode (second EOF) and the dipole-like mode (third EOF) suggests that the role exchange between the two Arctic atmospheric circulation modes observed before and after

the 2000s represents a statistically significant shift (table S2).

To evaluate the robustness of the explained variance associated with each mode derived from the observation-based EOF analysis, additionally, the Monte Carlo method, a widely used statistical testing approach, was applied [49, 50], thereby confirming the statistical significance and reliability of each EOF mode (table S3).

We further examine the variability of the three leading PC time series of Arctic atmospheric circulation related to ASI loss over the entire period from 1980 to 2022 (figures 2 and S7). As a result, the 11 year sliding variability of the third PC time series, associated with the dipole-like pattern of the third EOF mode, reveals a pronounced increase in Arctic atmospheric variability after the 2000s compared to the earlier period. While the variability remained consistently low with value less than 1 prior to 2000, it steadily increased thereafter, approaching a value near 2 in the post-2000s (figure 2(c)). In contrast, the 11 year sliding variability of the first PC time series, representing the AO-like pattern, showed similar magnitudes before and after 2000 (figure S7(b)). In the second PC time series, associated with the tripole-like pattern, variability increased to about 1.5 before 2000 but gradually declined thereafter (figure S7(d)). This contrasting behavior, together with the rise in variability of the dipole-like mode after 2000, suggests a reorganization of the dominant atmospheric circulation modes in the Arctic, likely driven by enhanced ASI variability. Since the 2000s, the dipole-like mode has emerged as the second leading mode, with indications that its increased variability could be contributing to changes in mid-latitude climate variability.

Here, we examine the relationship between the enhanced ASI variability and changes in NSHF variability since the 2000s, and their potential impacts on the increased variability of the dipole-like mode. As shown in figure S8, the 11 year sliding variance of ASI over the Arctic Ocean exhibits a sharp increase in the early 2000s, followed by a gradual decline. A similar temporal pattern is observed in NSHF variability over oceanic Arctic regions, with a significant TCC of 0.85 (99% confidence level). In contrast, NSHF variability over Arctic land areas remains relatively low and stable before the 2000s but increases sharply thereafter, closely mirroring the temporal evolution of the dipole-like mode's PC variability (TCC = 0.93, statistically significant at the 99% confidence level). Interpreted alongside the post-2000s trend pattern of NSHF (figure S4(c)), these results suggest that oceanic NSHF primarily reflects enhanced ocean heat uptake from the atmosphere, which is closely linked to the variability of the declining ASI. Conversely, land-based NSHF represents energy release from the land surface to the atmosphere, likely acting as a key driver of increased variability in Arctic atmospheric circulation, particularly in the dipole-like mode. These results provide observational evidence for the close coupling between ASI variability, surface heat fluxes, and atmospheric circulation, and their role in the observed shifts in Arctic atmospheric modes since the 2000s.

3.3. Enhanced variability in East Asian surface temperature

To assess the impact of increased variability in the dipole-like mode of Arctic atmospheric circulation on summer surface temperature variability in East Asia, we analyzed changes in temperature variability before and after the 2000s using the standard deviation metric (figures 3(a) and S9). The results reveal a clear and widespread increase in surface temperature variability across East Asia since the 2000s (figure 3(a)). This increase is most pronounced over inland China, while relatively weaker increases are seen in northeastern China, the Korean Peninsula, and Japan. This spatial pattern is also robust and consistently reproduced in results calculated using daily surface temperature data (figure S9). Although surface temperature variability over Mongolia was relatively high compared to surrounding regions, this signal is more likely attributable to local land–atmosphere interactions, particularly enhanced variability associated with soil moisture–temperature coupling, driven by the region's characteristic arid, inland conditions, rather than to large-scale influences from Arctic atmospheric circulation modes [51–53]. In severely arid regions, limited surface moisture amplifies the responsiveness of surface temperature, thereby increasing its variability.

To isolate the large-scale signal relevant to Arctic influence, we therefore excluded Mongolia, where such localized effects are especially pronounced, from the calculation of long-term surface temperature variability. Consequently, the 11 year sliding variance was computed over East Asia within the domain 25–40 °N and 100–140 °E (figure 3(b)). The 11 year sliding variability of summer surface temperatures over East Asia exhibits a pattern comparable to that of the Arctic dipole-like mode in figure 2(c), remaining relatively stable before the 2000s but showing a gradual upward trend thereafter (figure 3(b)). A temporal correlation analysis further revealed a strong association between this regional temperature variability and the 11 year sliding variance of the PC time series representing the dipole-like pattern, with a statistically significant correlation coefficient of 0.70 (99% confidence level). To assess the sensitivity of these results to the domain definition, we performed additional analyses using alternative East Asian domains with varying spatial extents (figure S10). The increase in post-2000 temperature variability and its strong linkage to the Arctic dipole-like mode are consistently reproduced across all domains, confirming that the identified relationship is robust and not sensitive to the specific choice

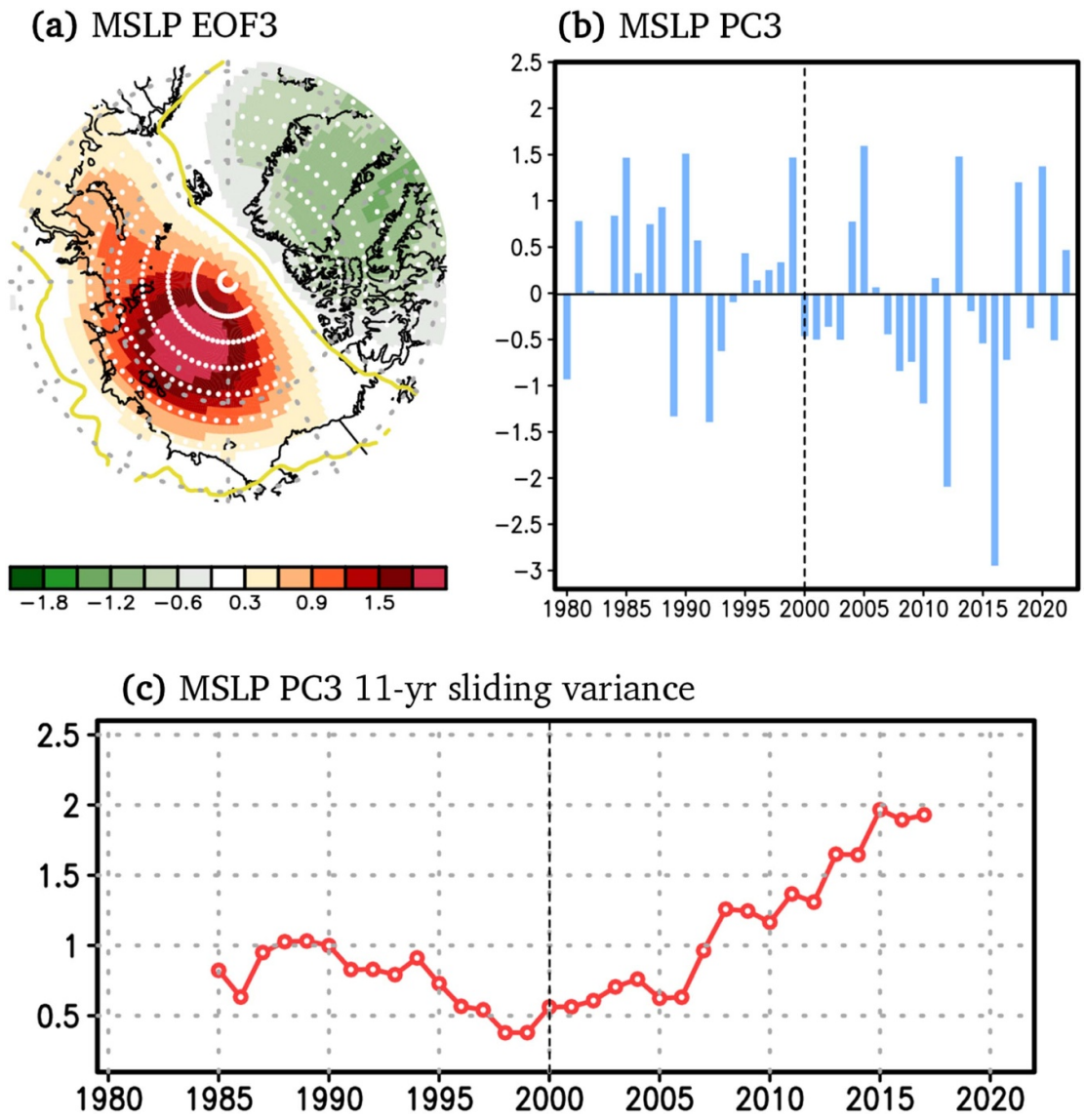


Figure 2. Dipole-like mode of summer Arctic atmospheric circulation and its enhanced ariability. (a) Observed regression pattern of JJA MSLP anomalies (65°–90 °N) onto the standardized principal component of the 3rd mode from EOF analysis of JJA MSLP anomalies. The EOF analysis is performed over 60°–90 °N with cosine-latitude weighting for 1980–2022. Stippled areas denote regions statistically significant at the 90% confidence level based on a two-tailed Student's *t*-test. The explained variance of EOF3 is 10.3%. (b) Corresponding principal component (PC3) time series. (c) 11 year sliding variance of the PC3 time series. The values are plotted at the central year of each 11 year sliding window.

of domain. These results imply that enhanced variability in the Arctic dipole-like mode may play a critical role in the recent intensification of summer surface temperature variability across East Asia.

3.4. Dynamical processes in enhancing East Asian surface temperature variability

Based on previous analysis, we investigate the specific dynamical processes through which the increased variability of the Arctic dipole-like circulation mode influences summer surface temperature variability in East Asia, with particular focus on the underlying physical mechanisms that mediate the teleconnection between the Arctic and the mid-latitudes.

The dipole-like mode of Arctic atmospheric circulation, characterized by a positive anomaly over the Laptev and the Eastern Siberian Seas and a negative anomaly near Greenland, demonstrates a statistically significant relationship with the meridional displacement of the East Asian jet stream. This linkage is most evident in the pronounced intensification of the meridional shift of the upper-level jet (figure 4(a)). Concurrently, distinct anomalous patterns appear in both the vertical and meridional wind fields, with enhanced upward motion between 35 °N and 45 °N and subsidence between 25 °N and 35 °N. These features collectively form a quasi-barotropic vertical

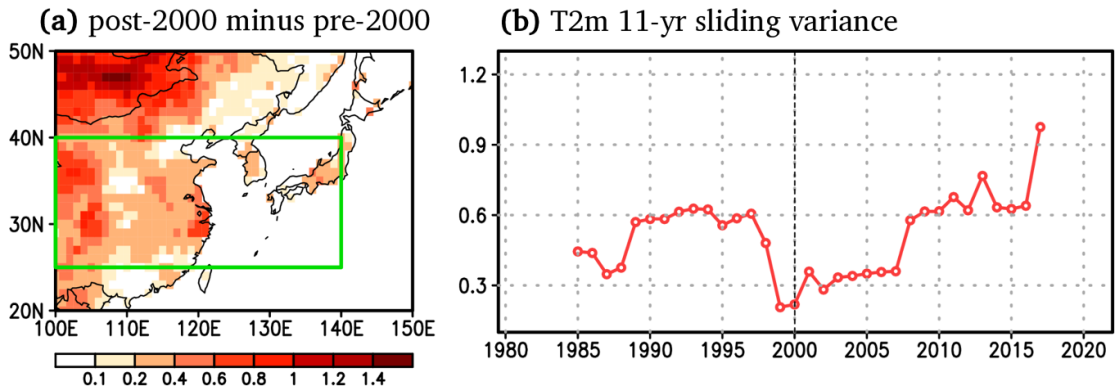


Figure 3. Variability of East Asian summer surface temperature. (a) Difference in the standard deviation of JJA mean 2 m air temperature (T2m, °C) between the post-2000s (2000–2022) and pre-2000s (1980–1999). The green box indicates the East Asian domain (25°–40 °N, 100°–140 °E) used for the area-averaged time series in panel (b). (b) 11 year sliding variance of the T2m time series averaged over East Asia (25°–40 °N, 100°–140 °E) for 1980–2022. The values are plotted at the central year of each 11 year sliding window.

structure (figure 4(b)). They are spatially aligned with the regions of jet stream intensification and weakening, indicating a dynamically coupled response between Arctic atmospheric variability and upper-tropospheric circulation over East Asia. Furthermore, the altered Arctic circulation also reshapes the meridional temperature gradient, producing a dipole structure with a strengthened gradient north of ∼40 °N and a weakened gradient to the south (figure 4(c)). This thermal contrast induces corresponding variations in the zonal wind field, consistent with the observed meridional displacement and intensification of the upper-level jet stream (figure 4(a)). In particular, convergence of the upper-level wind field near 30 °N induces strong subsidence, while divergence near 40 °N is accompanied by marked upward motion, producing a vertically coherent convergence–divergence structure (figures 4(b) and (d)). This vertical structure, influenced by the enhanced variability of the Arctic dipole-like mode since the 2000s, has a substantial dynamical influence on modulating the local atmospheric circulation over East Asia. Cyclonic anomalies and ascent at higher latitudes promote surface cooling, whereas anticyclonic anomalies and subsidence at lower latitudes lead to surface warming. These opposing effects intensify meridional temperature contrasts and variability across East Asia. As the variability of the Arctic dipole-like mode continues to intensify, the jet stream's meridional displacement becomes increasingly erratic, potentially inducing significant changes in the vertical structure and dynamical behavior of the East Asian atmosphere, deviating from its climatological mean state. Such changes, driven by Arctic sea-ice decline and an increased frequency of dipole-like events, are likely to further enhance the meridional variability of summer surface temperatures over East Asia, thereby increasing regional climate instability and the unpredictability of temperature extremes.

These dynamical processes indicate that the influence of the Arctic dipole-like mode on East Asian climate is not limited to regional circulation changes, but is also embedded within larger-scale atmospheric variability. The dipole-like mode is dynamically connected to broader Northern Hemisphere teleconnection patterns. Its structure is consistent with Arctic dipole–type variability [46, 54] and is associated with meridional pressure gradients that influence jet stream displacement. Previous studies have shown that Arctic circulation anomalies can interact with Eurasian wave trains and blocking activity, including Ural blocking, thereby modulating midlatitude climate variability [55–57]. Although these mechanisms have been primarily documented in winter, they provide a useful framework for interpreting Arctic–midlatitude linkages. Arctic variability has also been linked to changes in summertime atmospheric circulation, including enhanced meridional amplitude of large-scale waves [58, 59]. In this context, the dipole-like mode can be interpreted as part of a broader teleconnection framework influencing East Asian summer climate. Therefore, the enhanced variability of this mode since the 2000s reflects a reorganization of existing atmospheric variability under strengthened Arctic forcing, rather than the emergence of an independent circulation mode.

Building on this dynamical framework, our findings are consistent with previous studies highlighting the role of Eurasian teleconnection patterns in shaping East Asian summer extremes. For example, a recent study [60] showed that the relationship between heatwaves in the mid–lower reaches of the Yangtze River valley and upstream atmospheric wave trains has intensified since the 2000s. The Arctic dipole-like mode identified in this study modulates the meridional structure of the jet stream, which may influence downstream atmospheric variability across Eurasia. This suggests that Arctic-driven circulation

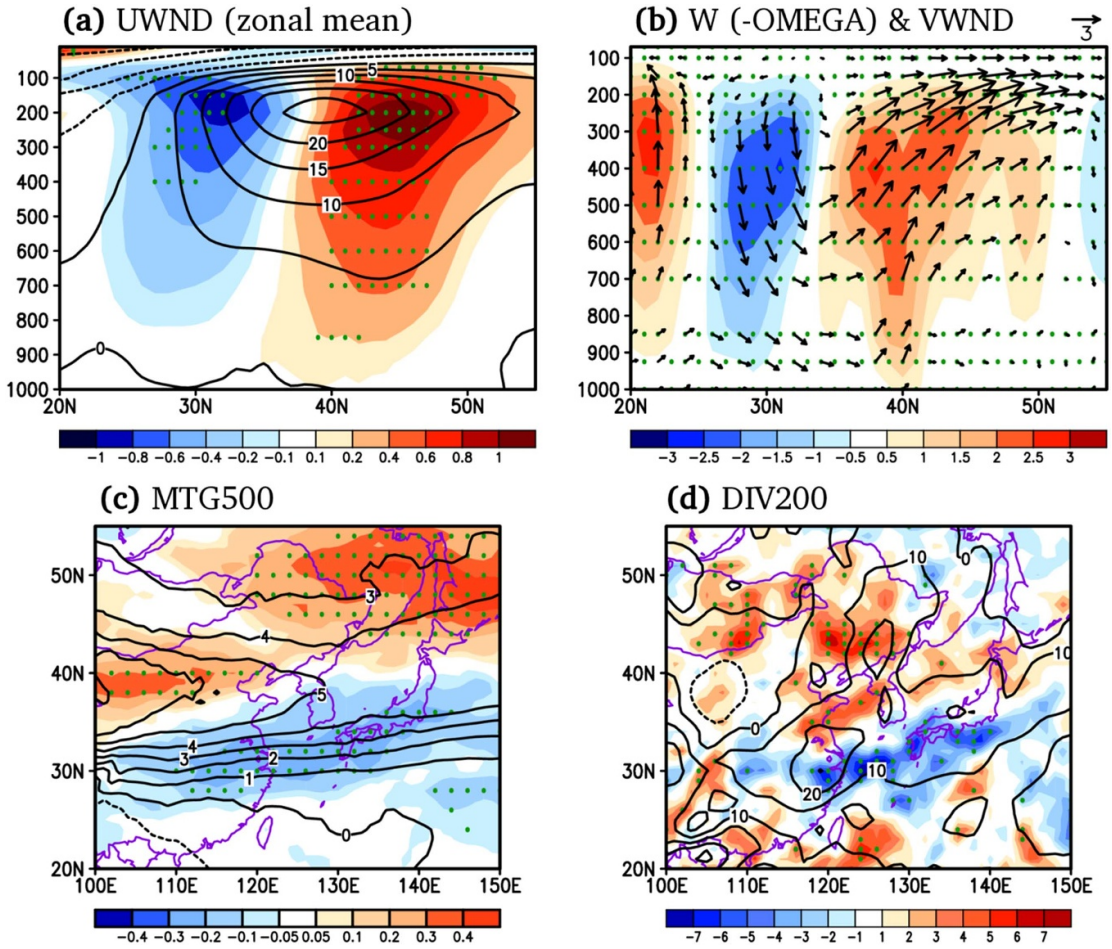


Figure 4. Atmospheric responses associated with the Arctic dipole-like mode. (a) Vertical cross-section (zonal mean over 100°–140 °E) of JJA zonal wind (UWND, m s^{-1}) anomalies regressed onto the standardized principal component of the 3rd EOF mode derived from JJA MSLP anomalies over 60°–90 °N (cosine-latitude weighted) for 1980–2022. Black contours show the climatological mean (m s^{-1}) for 1980–1999 over the same longitudinal band. (b), Same as (a), but for vertical velocity (shading, -OMEGA, $\times 10^{-3}$ Pa s^{-1}) and meridional wind (VWND, $\times 10^{-1}$ m s^{-1}). (c), Same as (a), but showing the regression pattern of the meridional temperature gradient at 500 hPa (MTG500, $\times 10^{-6}$ °C m^{-1}). (d), Same as (c), but for divergence at 200 hPa (DIV200, $\times 10^{-7}$ s^{-1}), where positive (negative) values indicate divergence (convergence). Black contours in (c) and (d) denote the climatological mean for 1980–1999. Stippling indicates statistical significance at the 90% confidence level based on a two-tailed Student's *t*-test.

changes and Eurasian teleconnection processes are dynamically linked, providing a physical basis for understanding enhanced variability of summer temperature extremes over East Asia.

3.5. Dipole-like mode reorganization induced by ASI decline: insights from coupled model experiments

We hypothesize that highly variable Arctic SSTs may have driven the observed ASI decline and its enhanced variability, which in turn contributed to the reorganization of Arctic circulation modes, as revealed by EOF analysis.

To directly test this hypothesis, we conduct two coupled model experiments with SST nudging using the GFDL-CM2.1 (see section 2 for details). The differences between the two experiments allow us to isolate the influence of observed Arctic SST anomalies on sea ice loss and the resulting reorganization of atmospheric circulation.

EOF analysis of simulated SLP difference anomalies reveals that, although the leading AO-like mode shows little structural change across periods, the higher-order modes undergo notable reorganization associated with ASI decline (figure S11). Specifically, the pre-2000 tripole-like pattern shifts to the third mode after 2000 and is replaced by a dipole-like structure as the second dominant circulation mode, consistent with observations (spatial correlation of 0.69; figures S6(h) and S11(h)). Relationships among these reorganized EOF patterns are summarized in table S4. Together, these results strongly suggest that ASI forcing plays a critical role in the strengthening and increased dominance of the dipole-like pattern as the leading circulation mode in recent decades. To further examine the robustness of the identified circulation modes, we performed additional EOF analysis using individual ensemble members (figure S12). The results show that the leading modes remain consistent across the total, pre-2000, and post-2000 periods,

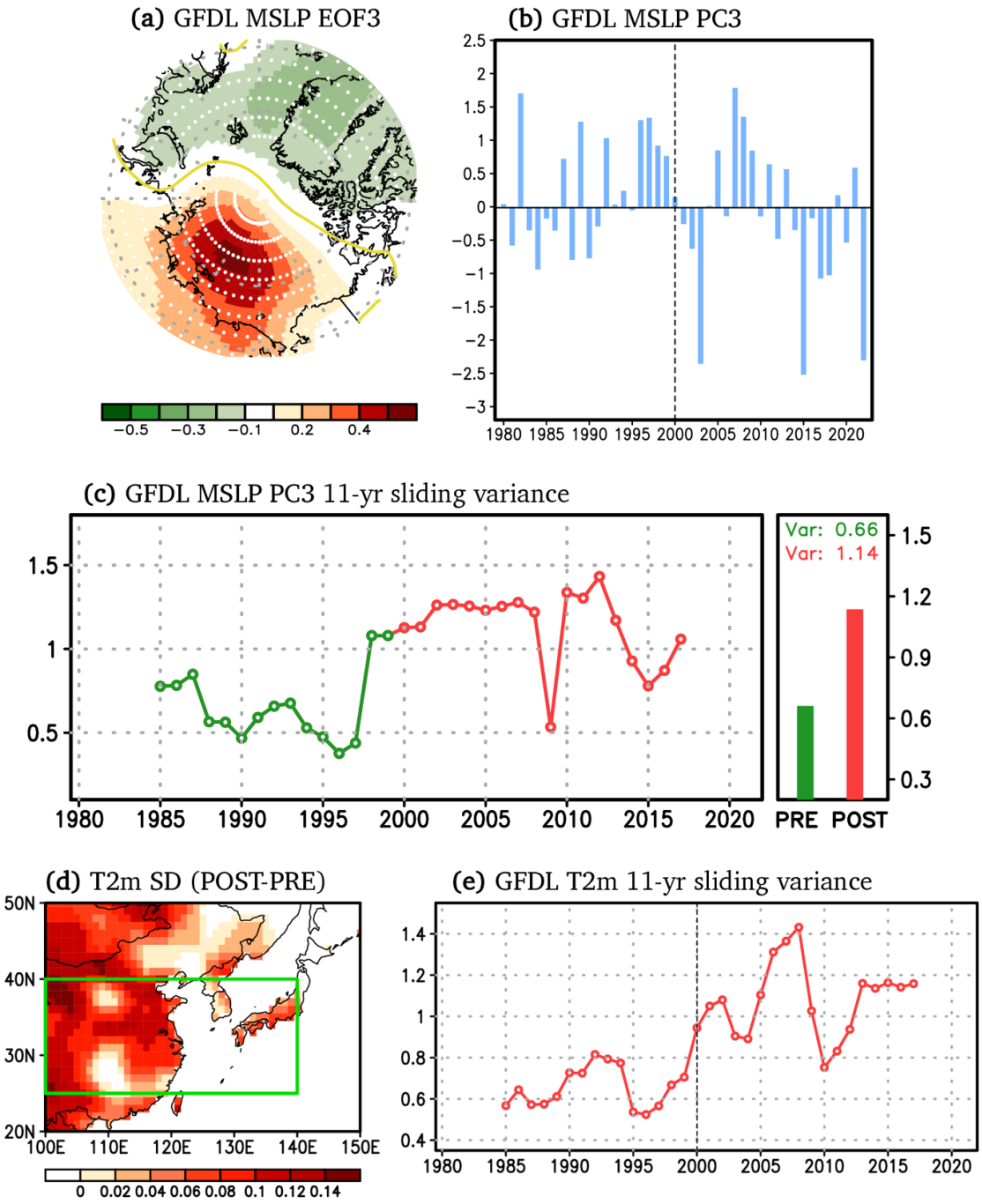


Figure 5. Arctic atmospheric dipole-like mode derived from SST-nudged GFDL simulations (ARCTIC_run—CLIM_run) and its linkage to East Asian temperature variability. (a) Regression pattern of JJA MSLP difference anomalies onto the standardized principal component of the 3rd mode, computed from EOF analysis of JJA SLP difference anomalies over 60°–90 °N using cosine-latitude weighting. The difference anomalies are obtained from the historical (ARCTIC_run) and climatological (CLIM_run) SST-nudged simulations for the full period (1980–2022). Stippling indicates statistical significance at the 90% confidence level (two-tailed Student's *t*-test). The 3rd EOF mode explains 11.5% of the total variance. (b) Corresponding principal component (PC3) time series for 1980–2022. (c) 11 year sliding variance of PC3, with mean values shown for pre-2000s (1980–1999) and post-2000s (2000–2022). (d) Difference in standard deviations (SDs) of 2 m air temperature (T2m, °C) between the post-2000s and pre-2000s, calculated from the T2m difference anomalies between the two SST-nudged simulations. The green box indicates the East Asian domain (25°–40 °N, 100°–140 °E) used for the area-averaged time series in panel (e). (e) 11 year sliding variance of simulated T2m averaged over East Asia (25°–40 °N, 100°–140 °E) for 1980–2022. The values are plotted at the central year of each 11 year sliding window.

with the dipole-like pattern persistently appearing as the second mode. This suggests that the dipole-like mode is an intrinsic feature of Arctic atmospheric variability, independent of the forcing strength. In contrast, the ensemble-mean EOF analysis exhibits a clear reordering of modes, with the dipole-like pattern increasing in relative importance during the post-2000 period. This discrepancy highlights the distinct roles of internal variability and externally forced signals. When internal variability is retained,

the modal hierarchy remains stable; however, when it is suppressed through ensemble averaging, the relative contribution of the forced signal becomes more pronounced.

To further assess whether the variability of the dipole-like mode intensifies over time, as implied by the observed third PC time series (figure 2), we compute 11 year sliding variances of the simulated third PCs for 1980–2022 (figure 5). The model's third EOF mode closely matches the observed dipole-like pattern, with a spatial correlation of 0.76 between figures 2(a) and 5(a). The third PC time series shows substantially greater variability after the 2000s, with the averaged sliding variance increasing from 0.66 to 1.14 (a factor of 1.73), confirming an intensification of Arctic atmospheric variability in the model (figure 5(c)). A transient reduction in variability around 2009 is also evident, which is attributable to internal variability and the finite length of the sliding window, and does not affect the overall increasing trend. The post-2000 increase in the variability of the simulated dipole-like mode is also consistent with the enhanced variability of simulated Arctic SIC and SST, in agreement with observations (figures S13 and S14). This suggests that amplified Arctic Ocean variability plays a central role in strengthening atmospheric variability over the region. Moreover, as shown in figures S15 and 5(d), (e), summer surface temperature variability over East Asia has markedly increased since the 2000s and exhibits a strong linkage to the third dipole-like mode of Arctic atmospheric variability (TCC between figures 5(c) and (e) = 0.59, 99% confidence level). These findings reinforce the observational conclusion that intensified variability of the Arctic dipole-like mode exerts an substantial influence on summer temperature variability over East Asia.

4. Conclusions and discussions

This study demonstrates that the enhanced interannual variability of East Asian summer surface temperature since the early 2000s is closely linked to increased variability in ASI concentration. This linkage is manifested through the strengthening and increased dominance of a dipole-like Arctic circulation mode, which reorganizes atmospheric variability and strengthens Arctic–midlatitude interactions. These structural changes in the Arctic atmosphere are not limited to mean state alterations but involve amplified variability in dominant circulation modes, leading to substantial impacts on upper-tropospheric dynamics and East Asian summer temperature variability. Such findings imply a strengthened Arctic–midlatitude teleconnection, whereby internal variability of the Arctic climate system may intensify midlatitude climate fluctuations and increase the likelihood of extreme events. It is important to note that our model experiments were driven solely by SST forcing, limiting the representation of fully coupled processes. Further research will be required to more comprehensively assess the underlying nonlinear mechanisms [61–63] governing the amplified variability of the dipole-like Arctic atmospheric circulation mode.

Crucially, our results indicate that the decline and increased variability of ASI during summer are not merely a regional feature but a fundamental driver of broader climate variability. Beyond East Asia, variability in ASI has the potential to modulate temperature and precipitation fluctuations across other midlatitude regions and even at the global scale through strengthened teleconnections. Importantly, the influence of ASI extends beyond mean-state shifts, directly shaping climate variability and thereby affecting the frequency and intensity of extremes. These findings suggest that ASI variability should be considered a critical element in future seasonal climate predictions and long-term risk assessments. Taken together, our findings underscore the need to reevaluate atmosphere-ocean–sea ice interactions within the climate system and may mark an important turning point in our understanding of Arctic–midlatitude, and more broadly Arctic–global, linkages.

Acknowledgments

D.Y.L. was supported by Basic Science Research Program through the National Research Foundation of Korea (NRF) funded by the Ministry of Education (RS-2023-00242438). S.-W.Y. is funded by the Korea Meteorological Administration Research and Development Program under Grant RS-2024-00403698.

Data availability statement

All data are available in the manuscript or the supplementary materials. ERSST v5 data on sea surface temperature (SST) can be downloaded from https://psl.noaa.gov/data/gridded/data.noaa.ersst.v5.html. Sea ice concentration (SIC) of NOAA/National Snow and Ice Data Center (NSIDC) can be downloaded from https://noaadata.apps.nsidc.org/NOAA/G02202_V4/north/aggregate/. The GFDL CM2.1 model and corresponding data are available from the GFDL portal server (https://data1.gfdl.noaa.gov/CM2.X).

The data that support the findings of this study are openly available at the following URL/DOI: https://www.ecmwf.int/en/forecasts/dataset/ecmwf-reanalysis-v5 [29].

Supplementary data 1 available at https://doi.org/10.1088/1748-9326/ae5fb0/data1.

ORCID iDs

Doo Young Lee 0000-0002-6129-2241
Sang-Wook Yeh 0000-0003-4549-1686
Shangfeng Chen 0000-0003-4347-8592
Renguang Wu 0000-0003-4712-2251

References

[1] Budikova D 2009 Role of Arctic sea ice in global atmospheric circulation: a review *Glob. Planet. Change* **68** 149–63
[2] Zhang X, He B, Bao Q, Liu Y, Wu G, Duan A, Hu W, Sheng C and Rao J 2024 The role of Arctic sea ice loss in the interdecadal trends of the East Asian summer monsoon in a warming climate *npj Clim. Atmos. Sci.* **7** 174
[3] Cvijanovic I *et al* 2025 Arctic sea-ice loss drives a strong regional atmospheric response over the North Pacific and North Atlantic on decadal scales *Commun. Earth Environ.* **6** 154
[4] Bhatt U S *et al* 2014 Implications of Arctic sea ice decline for the earth system *Annu. Rev. Environ. Resour.* **39** 57–89
[5] Cai Q, Wang J, Beletsky D, Overland J, Ikeda M and Wan L 2021 Accelerated decline of summer Arctic sea ice during 1850–2017 and the amplified Arctic warming during the recent decades *Environ. Res. Lett.* **16** 034015
[6] Chen P, Wang X, Zhao J, Li T, Shi J, Zong F and Wei L 2023 Variability of Arctic Sea ice age and its relationship with atmospheric circulation patterns *Front. Mar. Sci.* **10** 1274665
[7] Sumata H, de Steur L, Divine D V, Granskog M A and Gerland S 2023 Regime shift in Arctic Ocean sea ice thickness *Nature* **615** 443–9
[8] Deng J and Dai A 2022 Sea ice–air interactions amplify multidecadal variability in the North Atlantic and Arctic region *Nat. Commun.* **13** 2100
[9] Wu W and Dai H 2025 Roles of sea ice and seasonal heat storage in determining the seasonal Arctic surface warming are studied with CMIP6 simulations *Sci. Rep.* **15** 12216
[10] Duffey A, Mallett R, Irvine P J, Tsamados M and Stroeve J 2023 ESD Ideas: arctic amplification's contribution to breaches of the Paris agreement *Earth Syst. Dyn.* **14** 1165–9
[11] Liu X and Lu C 2021 Effects of sea ice change on the Arctic climate: insights from experiments with a polar atmospheric regional climate model *J. Water Clim. Change* **12** 2885–93
[12] Screen J A and Simmonds I 2010 The central role of diminishing sea ice in recent Arctic temperature amplification *Nature* **464** 1334–7
[13] Kim K-Y, Hamlington B D, Na H and Kim J 2016 Mechanism of seasonal Arctic sea ice evolution and Arctic amplification *Cryosphere* **10** 2191–202
[14] Hwang B and Landy J 2020 Impacts of climate change on Arctic sea ice *MCCIP Sci. Rev.* **2020** 208–27
[15] Ding Q *et al* 2017 Influence of high-latitude atmospheric circulation changes on summertime Arctic sea ice *Nat. Clim. Change* **7** 289–95
[16] Lee D Y, Yeh S-W, Lee Y-H, Cai W, Wang G and Yang Y-M 2025 The emergence of a dipole-like mode in Arctic atmospheric circulation conducive to European heat waves *Commun. Earth Environ.* **6** 81
[17] Budikova D, Ford T W and Ballinger T J 2019 United States heat wave frequency and Arctic Ocean marginal sea ice variability *J. Geophys. Res.* **124** 6247–64
[18] Narayanasetti S, Panickal S, Krishnan R, Mujumdar M, Samanta S and Ravichandran M 2025 Arctic sea-ice decline causes intense summer monsoon precipitation events over South Asia under greenhouse warming *Environ. Res. Lett.* **20** 054073
[19] Delhaye S, Fichefet T, Massonnet F, Docquier D, Msadek R, Chripko S, Roberts C, Keeley S and Senan R 2022 Summertime changes in climate extremes over the peripheral Arctic regions after a sudden sea ice retreat *Weather Clim. Dyn.* **3** 555–73
[20] Wu B and Francis J A 2019 Summer Arctic cold anomaly dynamically linked to East Asian heat waves *J. Clim.* **32** 1137–50
[21] Chen X, Dai A, Wen Z and Song Y 2021 Contributions of Arctic sea-ice loss and East Siberian atmospheric blocking to 2020 record-breaking Meiyu-Baiu rainfall *Geophys. Res. Lett.* **48** e2021GL092748
[22] Wu B, Zhang R, Wang B and D'Arrigo R 2009 On the association between spring Arctic sea ice concentration and Chinese summer rainfall *Geophys. Res. Lett.* **36** L09501
[23] Liu Y, Zhang Y, Gu S, Yang X-Q and Zhang L 2023 A cross-seasonal linkage between Arctic sea ice and Eurasian summertime temperature fluctuations *Adv. Atmos. Sci.* **40** 2195–210
[24] Chen R, Wen Z, Lu R and Liu W 2021 Interdecadal changes in the interannual variability of the summer temperature over Northeast Asia *J. Clim.* **34** 8361–76
[25] Mallett R D C, Stroeve J C, Tsamados M, Landy J C, Willatt R, Nandan V and Liston G E 2021 Faster decline and higher variability in the sea ice thickness of the marginal Arctic seas when accounting for dynamic snow cover *Cryosphere* **15** 2429–50
[26] Serreze M C and Stroeve J 2015 Arctic sea ice trends, variability and implications for seasonal ice forecasting *Phil. Trans. R. Soc. A* **373** 20140159
[27] Deser C, Walsh J E and Timlin M S 2000 Arctic sea ice variability in the context of recent atmospheric circulation trends *J. Clim.* **13** 617–33
[28] Sim J-H, Kim B-M, Lee J-G, Lim Y-K, Kim J-H and Kim J H 2025 Sea ice initialization and its impact on winter seasonal prediction skill over the northern hemisphere in coupled forecast system *J. Clim.* **38** 3989–4001
[29] Hersbach H, Bell B, Berrisford P, Hirahara S, Horányi A, Muñoz-Sabater J, Nicolas J, Peubey C, Radu R and Schepers D 2020 The ERA5 global reanalysis *Q. J. R. Meteorol. Soc.* **146** 1999–2049
[30] Huang B, Thorne P W, Banzon V F, Boyer T, Chepurin G, Lawrimore J H, Menne M J, Smith T M, Vose R S and Zhang H M 2017 NOAA extended reconstructed sea surface temperature (ERSST) version 5 *NOAA National Centers for Environmental Information* vol 30 pp 25
[31] Peng G, Meier W N, Scott D and Savoie M 2013 A long-term and reproducible passive microwave sea ice concentration data record for climate studies and monitoring *Earth Syst. Sci. Data* **5** 311–8
[32] Rodionov S N 2004 A sequential algorithm for testing climate regime shifts *Geophys. Res. Lett.* **31** L09204
[33] Pettitt A N 1979 A non-parametric approach to the change-point problem *J. R. Stat. Soc. C* **28** 126–35
[34] Quadrelli R, Bretherton C S and Wallace J M 2005 On sampling errors in empirical orthogonal functions *J. Clim.* **18** 3704–10
[35] Zhang X, Wu B and Ding S 2024 Summer Russian heat waves linked to Arctic Sea ice anomalies in 2010 and 2016 *J. Clim.* **37** 1597–611
[36] Delworth T L *et al* 2006 GFDL's CM2 global coupled climate models *J. Clim.* **19** 643–74
[37] Rinke A, Handorf D, Dorn W, Dethloff K, Moore J C and Zhang X 2018 Atmospheric feedbacks on Arctic summer sea-ice anomalies in ensemble simulations of a coupled regional climate model *Adv. Polar Sci.* **29** 156–64
[38] Screen J A, Deser C and Sun L 2015 Reduced risk of North American cold extremes due to continued Arctic sea ice loss *Bull. Am. Meteorol. Soc.* **96** 1489–503

[39] Deser C, Tomas R A and Sun L 2015 The role of ocean–atmosphere coupling in the zonal-mean atmospheric response to Arctic sea ice loss *J. Clim.* **28** 2168–86
[40] Smith T M, Reynolds R W, Peterson T C and Lawrimore J 2008 Improvements to NOAA's historical merged land–ocean surface temperature analysis (1880–2006) *J. Clim.* **21** 2283–96
[41] Kim H, Yeh S-W, An S-I, Park J-H, Kim B-M and Baek E-H 2020 Arctic sea ice loss as a potential trigger for central Pacific El Niño events *Geophys. Res. Lett.* **47** e2020GL087028
[42] Song S-Y, Yeh S-W, Kim H and Holbrook N J 2023 Arctic warming contributes to increase in Northeast Pacific marine heatwave days over the past decades *Commun. Earth Environ.* **4** 25
[43] Brownlee K A 1965 *Statistical Theory and Methodology in Science and Engineering* (A Wiley Publication in Applied Statistics)
[44] Tjernström M *et al* 2015 Warm-air advection, air mass transformation and fog causes rapid ice melt *Geophys. Res. Lett.* **42** 5594–602
[45] Thompson D W and Wallace J M 1998 The Arctic Oscillation signature in the wintertime geopotential height and temperature fields *Geophys. Res. Lett.* **25** 1297–300
[46] Wu B, Wang J and Walsh J E 2006 Dipole anomaly in the winter Arctic atmosphere and its association with sea ice motion *J. Clim.* **19** 210–25
[47] Screen J A, Bracegirdle T J and Simmonds I 2018 Polar climate change as manifest in atmospheric circulation *Curr. Clim. Change Rep.* **4** 383–95
[48] Wang J and Ikeda M 2000 Arctic oscillation and Arctic sea-ice oscillation *Geophys. Res. Lett.* **27** 1287–90
[49] Xiao-feng L, Pietrafesa L, Shu-Fang L and Li-an X 2000 Significance test for empirical orthogonal function (EOF) analysis of meteorological and oceanic data *J. Oceanol. Limnol.* **18** 10–17
[50] Wilks D S 2016 Modified "rule N" procedure for principal component (EOF) truncation *J. Clim.* **29** 3049–56
[51] Seo Y-W and Ha K-J 2022 Changes in land-atmosphere coupling increase compound drought and heatwaves over northern East Asia *npj Clim. Atmos. Sci.* **5** 100
[52] Li K, Zhang J, Yang K and Wu L 2019 The role of soil moisture feedbacks in future summer temperature change over East Asia *J. Geophys. Res.* **124** 12034–56
[53] Seneviratne S I, Lüthi D, Litschi M and Schär C 2006 Land–atmosphere coupling and climate change in Europe *Nature* **443** 205–9
[54] Overland J E and Wang M 2010 Large-scale atmospheric circulation changes are associated with the recent loss of Arctic sea ice *Tellus A* **62** 1–9
[55] Honda M, Inoue J and Yamane S 2009 Influence of low Arctic sea-ice minima on anomalously cold Eurasian winters *Geophys. Res. Lett.* **36** L08707
[56] Inoue J, Hori M E and Takaya K 2012 The role of Barents Sea ice in the wintertime cyclone track and emergence of a warm-Arctic cold-Siberian anomaly *J. Clim.* **25** 2561–8
[57] Luo D, Xiao Y, Diao Y, Dai A, Franzke C L and Simmonds I 2016 Impact of Ural blocking on winter warm Arctic–cold Eurasian anomalies. Part II: the link to the North Atlantic oscillation *J. Clim.* **29** 3949–71
[58] Screen J A and Simmonds I 2013 Exploring links between Arctic amplification and mid-latitude weather *Geophys. Res. Lett.* **40** 959–64
[59] Coumou D, Lehmann J and Beckmann J 2015 The weakening summer circulation in the Northern Hemisphere mid-latitudes *Science* **348** 324–7
[60] Shi J, Yao Y, Guo R, Luo B and Zhong L 2025 The intensifying relationship between heatwaves in the mid–lower reaches of the Yangtze River valley and the upstream atmospheric wave train after the 2000s *Atmos. Res.* **313** 107770
[61] Zhang W and Luo D 2020 A nonlinear theory of atmospheric blocking: an application to Greenland blocking changes linked to winter Arctic sea ice loss *J. Atmos. Sci.* **77** 723–51
[62] Alexander M A, Bhatt U S, Walsh J E, Timlin M S, Miller J S and Scott J D 2004 The atmospheric response to realistic Arctic sea ice anomalies in an AGCM during winter *J. Clim.* **17** 890–905
[63] Wettstein J J and Deser C 2014 Internal variability in projections of twenty-first-century Arctic sea ice loss: role of the large-scale atmospheric circulation *J. Clim.* **27** 527–50